ICIC Express Letters
Volume **11**, Number **11**, November **2017**
 ISSN 1881-803X
pp. **1635–1641**

A NOVEL CABLE DETECTION METHOD BASED ON COMBINED ALGORITHM OF EXTENSIVE NEURAL NETWORK AND CHAOS THEORY

Shiue-Der Lu[1], Meng-Hui Wang[2,*] and Kun-De Lin[2]

[1]Department of Electrical Engineering
Chung Yuan Christian University
No. 200, Chung Pei Rd., Chung Li Dist., Taoyuan City 320, Taiwan
SDL@cycu.edu.tw

[2]Department of Electrical Engineering
National Chin-Yi University of Technology
No. 35, Lane 215, Sec. 1, Chung-Shan Rd., Taiping Dist., Taichung City 411, Taiwan
*Corresponding author: wangmh@ncut.edu.tw

Received May 2017; accepted August 2017

Abstract. *This paper presents a method for accurately identifying the locations of leaks in gas-filled cables. Chaos eyes derived through chaos theory were computed, and the Chaos eyes were used as the features. An extensive neural network (ENN) was used to diagnose faults in gas-filled cables. Raw data were collected from a foam-skin polyethylene insulated Stalpeth sheathed cable system that was operated by Chunghwa Telecom Company, the largest telecommunications firm in Taiwan. The results suggested that the proposed method enabled the high accuracy identification of cable leaks and compared favorably to the traditional pressure gradient method in leak identification.*
Keywords: Gas-filled cables, Chaos eyes, Chaos theory, Extensive neural network, Diagnose faults, Foam-skin polyethylene insulated Stalpeth sheathed (F.S.-STP) cable, Traditional pressure gradient method

1. **Introduction.** Chunghwa Telecom, the largest telecommunications firm in Taiwan, detects leaks in gas-filled cables in accordance with its self-designed training materials concerning indoor gas-filled cables [1]. Specifically, the firm implements the traditional pressure gradient method (TPGM), which is a conventional leak detection method. Although the TPGM involves simple calculation, it is prone to error, which wastes time, money, and manpower for repairing gas-filled cables; additionally, the resulting delay in repair work can damage the insulation of the cables, leading to serious malfunctions in [2].

Some studies have conducted fault detection on cables. In [3], time difference-of-arrival was performed to detect faults in 11 kV-medium-voltage ethylene propylene rubber (EPR) cables. A chaotic analysis was conducted in [4] to identify insulation defects in high-voltage, direct current superconducting cables. In [5], resonant frequency analysis and PSCAD were used to conduct an online diagnosis of power cables. Other studies have applied algorithms for cable diagnosis. A partial discharge detection algorithm and a verification test were developed in [6] to locate faults in extra-high-voltage cables, and the algorithm was tested using a 154-kV cross-linked polyethylene (XLPE) power cable. In [7], an incipient fault location algorithm was proposed, which accounted for fault arc voltage and could detect fault locations in underground cables. Genetic algorithms were implemented in [8] to identify optimal connecting points between power lines and underground cables, thus reducing the impact of magnetic flux density. In [9], extension neural network (ENN) [10] was utilized to categorize and identify faults in internal combustion engines. An ENN-based diagnosis system was proposed in [11] to diagnose incipient faults

in power transformers and the method was tested using 40 dissolved gas analysis datasets from power transformers.

However, few studies have discussed fault detection or algorithm-based fault diagnosis in gas-filled cables. Thus, the present study used an ENN and chaos theory to detect leak locations in gas-filled cables. The ENN was designed to have a simple structure, simple compilation, and high accuracy rate. Moreover, preprocessing raw data by using chaos theory helped to enhance the ENN's fault-identification capability because the chaos theory has the ability to reduce a large number of original data into few important representative feature numbers.

The remainder of this paper is organized as follows. Section 2 presents the structure of F.S.-STP cable system. Section 3 describes the chaos theory and ENN fault detection method. Section 4 shows the performance of the proposed method and compares the results with different data. Finally, a brief conclusion is drawn.

2. **The Structure of F.S.-STP Cable System.** F.S.-STP cable is mainly designed for foam skin polyethylene insulated, aluminum and steel tape shield, polyethylene sheathed, (Stalpeth) local cable that is used for trunk between telephone offices and feeding between telephone offices and subscribers. Chunghwa Telecom's subscriber cable system uses a continuous-feed pipeline pressure system to fill F.S.-STP cables with air (Figure 1). The pipeline pressure system comprises a gas-filled cable, nitrogen inflator, air panel board, barrier, and air pressure sensor. The system uses the inflator to provide dry air with a relative humidity of 3% at 20°C into cables at a given pressure of 650 g/cm^2 or not higher than 9 psi), thus maintaining a certain pressure (typically 300 g/cm^2 (4 psi)) within the cables.

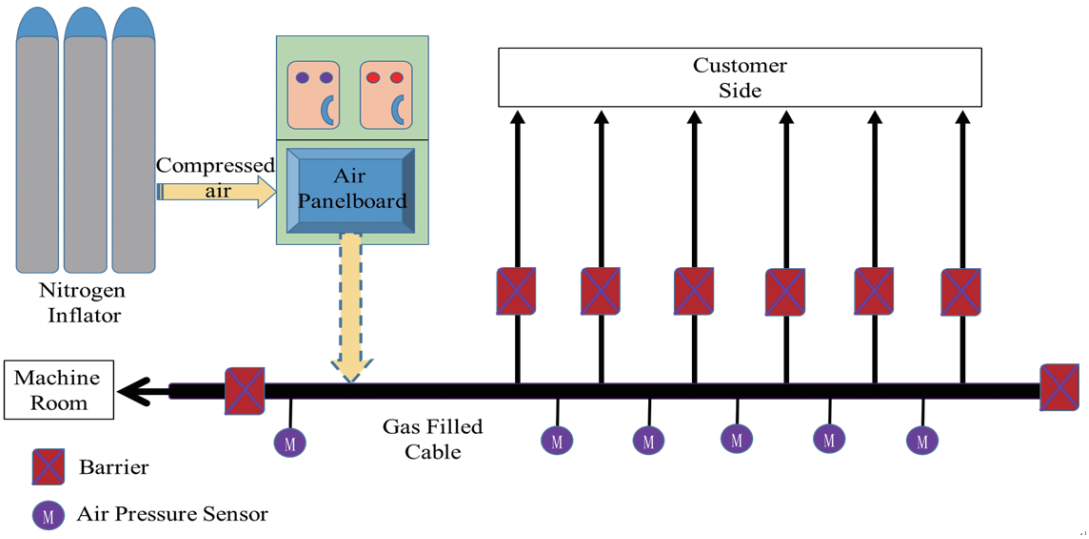

FIGURE 1. The structure of F.S.-STP cable system

3. **Methodology.**

3.1. **Chaos theory.** The chaotic dynamic error system extracts the dynamic errors between two chaos systems; the Lorenz chaos system is employed in this study. The master (L_{master}) and slave (L_{slave}) Lorenz systems are expressed in Equations (1) and (2), respectively.

$$L_{master} = \begin{cases} \dot{x_1} = \alpha(x_2 - x_1) \\ \dot{x_2} = \beta x_1 - x_1 x_3 - x_2 \\ \dot{x_3} = x_1 x_2 - \gamma x_3 \end{cases} \tag{1}$$

$$L_{slave} = \begin{cases} \dot{y_1} = \alpha(y_2 - y_1) \\ \dot{y_2} = \beta y_1 - y_1 y_3 - y_2 \\ \dot{y_3} = y_1 y_2 - \gamma y_3 \end{cases} \tag{2}$$

By subtracting Equations (1) and (2), the chaotic dynamic function of Lorenz master/slave system is obtained in the form of metric shown as Equation (3) [13].

$$\begin{bmatrix} \dot{e_1} \\ \dot{e_2} \\ \dot{e_3} \end{bmatrix} = \begin{bmatrix} -\alpha & \alpha & 0 \\ \beta & -1 & 0 \\ 0 & 0 & -\gamma \end{bmatrix} \begin{bmatrix} e_1 \\ e_2 \\ e_3 \end{bmatrix} + \begin{bmatrix} y_2 y_3 - x_2 x_3 \\ -y_1 y_3 + x_1 x_3 \\ y_1 y_2 - x_1 x_2 \end{bmatrix} \tag{3}$$

where x is the master system with an initial value of zero; y is the slave system containing original signal values; α, β, γ are the adjusted error coefficients and are based on the Lorenz's experimental experience which are set as 10, 28 and 8/3 respectively. e_1 and e_2 are used to generate the dynamical map of chaotic dynamic error. The coordinates of the two centers of gravity in the map are defined as the Chaos eyes, used as the features of the data of F.S.-STP leakage points [14,15].

3.2. **ENN fault detection method.** The ENN can be seen as supervised learning; the purpose of learning is to tune the weights of the ENN to achieve good clustering performance or to minimize the clustering error [11]. The schematic structure of the ENN is depicted in Figure 2. Before the learning, several variables have to be defined. Let training set be $\{X_1, T_1\}, \{X_2, T_2\}, \ldots, \{X_Q, T_Q\}$, where Q is the total number of training patterns, X_i is an input vector to the neural network and T_i is the corresponding target output. The i-th input vector is $X_i \equiv \{x_{i1}, x_{i2}, \ldots, x_{in}\}$, where n is the total number of the features. To evaluate the learning performance, the error function is defined below:

$$E_t = \frac{1}{2} \sum_{i=1}^{Q} \sum_{j=1}^{n_c} (t_{ij} - O_{ij})^2 \tag{4}$$

where t_{ij} represents the desired j-th output for the i-th input pattern, and O_{ij} represents the actual *j-th* output for the i-th input pattern.

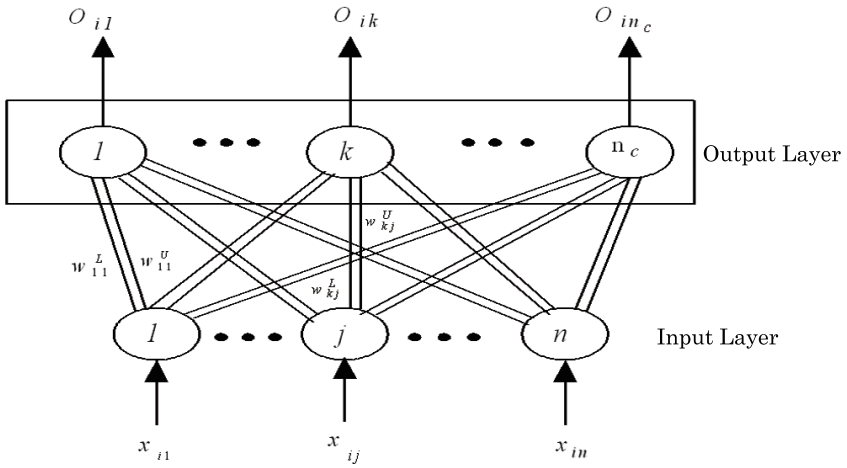

FIGURE 2. The structure of extension neural network (ENN)

The learning algorithm can be described as follows.

Step 1: Set the connection weights between input nodes and output nodes according to the range of classical domains. The range of classical domains can be directly obtained from previous experience, or determined from training data as follows:

$$w_{kj}^{L} = \min_{T_i \in k} \{x_{ij}\} \tag{5}$$

$$w_{kj}^{U} = \max_{T_i \in k} \{x_{ij}\} \tag{6}$$

$$\text{For } i = 1, 2, \ldots, Q; \quad j = 1, 2, \ldots, n; \quad k = 1, 2, \ldots, n_c$$

Step 2: Read the i-th training pattern and its cluster number p

$$X_i = \{x_{i1}, x_{i2}, \ldots, x_{in}\} \tag{7}$$

Step 3: Use the extension distance (ED) to calculate the distance between the input pattern X_i and the k-th cluster as follows:

$$ED_{ik} = \sum_{j=1}^{n} \left(\frac{\left| x_{ij} - \left(w_{kj}^{U} + w_{kj}^{L} \right) /2 \right| - \left(w_{kj}^{U} - w_{kj}^{L} \right) /2}{\left(w_{kj}^{U} - w_{kj}^{L} \right) /2} + 1 \right) \tag{8}$$

$$\text{For } k = 1, 2, \ldots, n_c$$

The proposed extension distance is a distance measurement; it can be graphically presented as in Figure 3. The proposed ED can describe the distance between the x and a range $\langle w^L, w^U \rangle$, which is different from the traditional Euclidean distance. We can see that different ranges of classical domains can arrive at different distances due to different sensitivities. This is a significant advantage in classification applications. Usually, if the feature covers a large range, the data requirement is fuzzy or low in sensitivity to distance. On the other hand, if the feature covers a small range, the data precision requirement and sensitivity to distance are high.

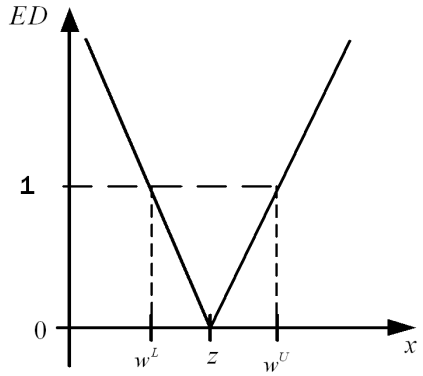

FIGURE 3. The proposed extension distance (ED)

Step 4: Find the m, such that $ED_{im} = \min \{ED_{ik}\}$. If $m = p$, then go to Step 6; otherwise go to Step 5.

Step 5: Update the weights of the p-th and the m-th clusters as follows:

$$\begin{cases} w_{pj}^{L(new)} = w_{pj}^{L(old)} + \eta \left(x_{ij} - \dfrac{w_{pj}^{L(old)} + w_{pj}^{U(old)}}{2} \right) \\ w_{pj}^{U(new)} = w_{pj}^{U(old)} + \eta \left(x_{ij} - \dfrac{w_{pj}^{L(old)} + w_{pj}^{U(old)}}{2} \right) \end{cases} \tag{9}$$

$$\begin{cases} w_{mj}^{L(new)} = w_{mj}^{L(old)} - \eta \left(x_{ij} - \dfrac{w_{mj}^{L(old)} + w_{mj}^{U(old)}}{2} \right) \\ w_{mj}^{U(new)} = w_{mj}^{U(old)} - \eta \left(x_{ij} - \dfrac{w_{mj}^{L(old)} + w_{mj}^{U(old)}}{2} \right) \end{cases} \tag{10}$$

$$\text{For } j = 1, 2, \ldots, n_c$$

where η is a learning rate, set to 0.1 in this paper. From this step, we can clearly see that the learning process is only to adjust the weights of the p-th and the m-th clusters.

Step 6: Repeat Step 2 to Step 5; if all patterns have been classified, then a learning epoch is finished.

Step 7: Stop, if the clustering process has converged, or the total error has arrived at a preset value; otherwise, return to Step 3.

It should be noted that the proposed ENN can take human expertise before the learning, and it can also produce meaningful output after the learning, because the classified boundaries of the features are clearly determined.

4. Simulation Results and Discussion.

4.1. **Experimental data.** Data were collected from Chunghwa Telecom's engineering projects. The gas-filled cable tested in this study, which was installed in a regional Internet data center in Taichung in central Taiwan, measured 1,652 m in length. Four pressure transducers were installed respectively in the data center, 87 m, 659 m, and 1,333 m away from the facility to detect leakage in the cable. Figure 4 presents a graph of different types of fault identified on the basis of testing data [2]. The figure suggests that the four features of the seven faults ranged from 3 to 7 and overlapped with each other. This caused reductions in the fault identification accuracy of an ENN during its training and identification. Thus, before the ENN was implemented, raw data were preprocessed to determine the features of each type of fault. The whole process of ENN and chaos

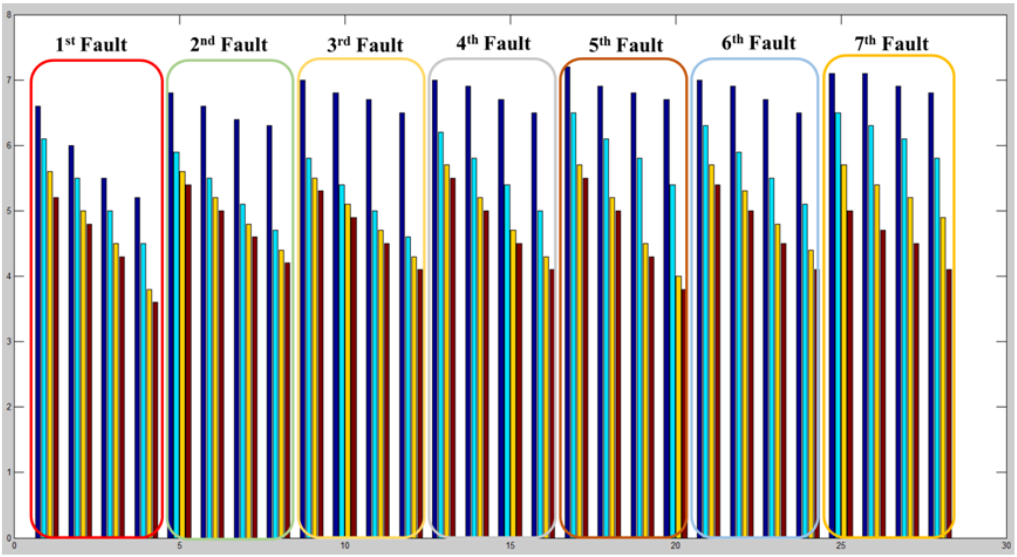

FIGURE 4. The curve of four manholes data

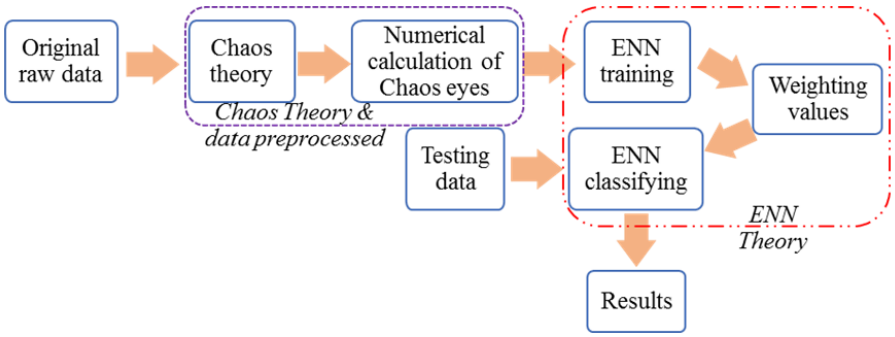

FIGURE 5. The whole process of ENN and chaos theory

theory shows in Figure 5. Firstly, chaos theory was used to calculate the features of the 28 raw data records to derive chaos eyes. Secondly, the coordinates of the Chaos eyes were multiplied, and their product was used as a feature. Thirdly, the ENN was trained with data obtained through preprocessing to get weighting values. Finally, the ENN identified leak locations (fault types) in the gas-filled cable from testing data.

4.2. **Testing results.** MATLAB was adopted to create algorithms of the chaos theory and ENN. Firstly, 28 raw data records were computed by using chaos theory to derive the Chaos eyes. The product of these Chaos eyes was used as the feature of each type of fault (Figure 6). Secondly, the ENN was trained with the 28 preprocessed data records, and the network was used to identify a randomly chosen preprocessed data record. The results of simulation with the ENN and the TPGM were compared, and the accuracies of ENN and TPGM are 85.7% and 43%, respectively. The proposed method has higher recognition accuracy than the TPGM [2]. Thirdly, having been identified by the ENN before and after preprocessing, the raw data were presented in the form of median and standard deviation and subsequently identified by the network. To take account of the noise and uncertainties, 28 sets of testing data were created by adding ±10% to ±30% of randomness, and the results are shown in Table 1. The proposed method has a significantly higher recognition accuracy of 82.4% with ±10% errors added. Contrarily, the accuracies of the other methods are only 25.9%, 22.6% and 17.4% under the same conditions. The accuracy rate of the proposed method is still higher than 66% even the noise errors added ±30% compared to other situation.

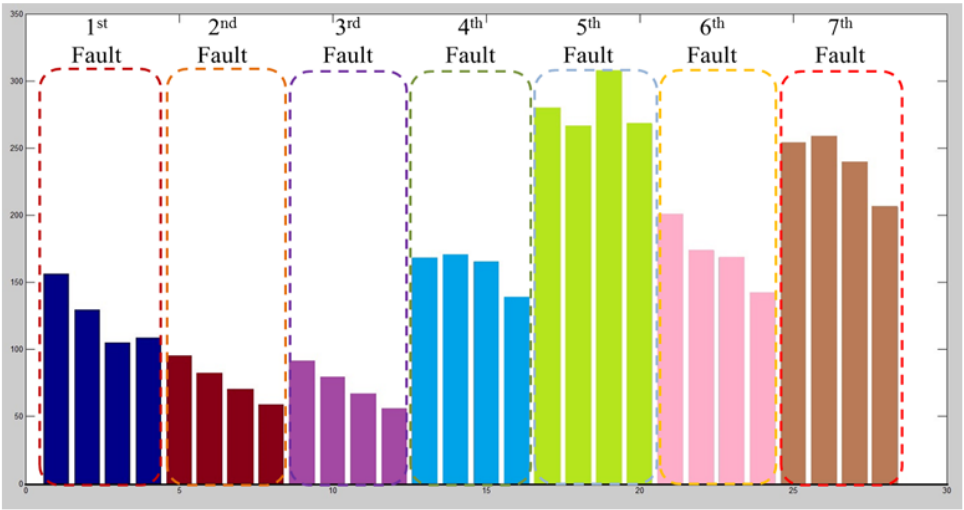

FIGURE 6. The preprocessing data of F.S.-STP leakage points by chaos method

TABLE 1. Diagnosis performances of errors added

Noise percentage	Raw data Accuracy rate	Raw data (Standard Deviation) Accuracy rate	Raw data (Median) Accuracy rate	Preprocessing data (Chaos eyes product) Accuracy rate	TPGM [2]
±0%	28.6%	28.6%	28.6%	**85.7%**	43%
±10%	25.9%	22.6%	17.4%	**82.4%**	N/A
±20%	24.1%	19%	15.7%	**75.3%**	N/A
±30%	21.9%	15.6%	12.3%	**66.7%**	N/A

5. **Conclusions.** A method for ensuring high-accuracy leak detection in gas-filled cables was developed in this study. An ENN was used to identify leak locations in a gas-filled cable. Measured data were preprocessed through chaos theory to derive Chaos eyes. The product of these Chaos eyes was applied in the training of the ENN to identify leaks in the cable. The simulation results indicated that the ENN was highly accurate compared with the TPGM, as well as when raw data were not preprocessed or when the medians and standard deviations of the data were estimated. The ENN achieved an identification rate of up to 79% even with the addition of a 10%, 20%, or 30% error signal. Moreover, the ENN had an identification rate that was three times without preprocessing and twice that of the TPGM. A fault diagnosis model for gas-filled cables was developed. The model can be used to extend the fault-diagnosis length of the cables as more measurement points are established or to diagnose faults in different types of cables and related devices.

REFERENCES

[1] *A Training Book for the Foam-Skin Polyethylene Insulated Stalpeth Sheathed Cable*, Directorate General of Telecommunications, 1988.

[2] S. S. Hung, K. C. Liao and A. P. Hung, The faulty diagnosis research of the cable's air leakage, *The 26th Power System Engineering Symposium*, Taiwan, pp.1206-1210, 2005.

[3] A. J. Reid, C. Zhou, D. M. Hepburn, M. D. Judd, W. H. Siewand and P. Withers, Fault location and diagnosis in a medium voltage EPR power cable, *IEEE Trans. Dielectrics and Electrical Insulation*, vol.20, no.1, pp.10-18, 2012.

[4] I. J. Seo, U. A. Khan, J. S. Hwang, J. G. Lee and J. Y. Koo, Identification of insulation defects based on chaotic analysis of partial discharge in HVDC superconducting cable, *IEEE Trans. Applied Superconductivity*, vol.25, no.3, 2015.

[5] Y. Kim and K. E. Holbert, New passive methodology for online power cable diagnosis by frequency analysis, *IEEE Power & Energy Society General Meeting*, pp.1-5, 2015.

[6] W. Choi, J. T. Kim, I. J. Seo, J. S. Hwang and J. Y. Koo, Development of a partial discharge detection algorithm and verification test for extra-high voltage cable system, *IET Science, Measurement & Technology*, vol.10, no.2, pp.111-119, 2016.

[7] S. Kulkarni, S. Santoso and T. A. Short, Incipient fault location algorithm for underground cables, *IEEE Trans. Smart Grid*, vol.5, no.3, pp.1165-1174, 2014.

[8] K. Horak, Optimal connection of power transmission lines with underground power cables to minimize magnetic flux density using genetic algorithms, *IEEE Trans. Power Delivery*, vol.23, no.3, pp.1553-1560, 2008.

[9] Y. Shatnawi and M. Al-khassaweneh, Fault diagnosis in internal combustion engines using extension neural network, *IEEE Trans. Industrial Electronics*, vol.61, no.3, pp.1434-1443, 2014.

[10] M. H. Wang and C. P. Hung, Extension neural network, *Neural Networks*, vol.16, pp.779-784, 2003.

[11] M. H. Wang, Extension neural network for power transformer incipient fault diagnosis, *IEE Proceedings – Generation on Transmission and Distribution*, vol.150, no.6, pp.679-685, 2003.

[12] H. J. C. Huijberts, H. Nijmeijer and R. M. A. Willems, System identification in communication with chaotic systems, *IEEE Trans. Circuits and Systems I: Fundamental Theory and Applications*, vol.20, pp.800-808, 2000.

[13] C. H. Huang, C. H. Lin and C. L. Kuo, Chaos synchronization-based detector for power-quality disturbances classification in a power system, *IEEE Trans. Power Delivery*, vol.26, no.2, pp.944-953, 2010.

[14] H. T. Yau and M. H. Wang, Chaotic eye-based fault forecasting method for wind power systems, *IET Renewable Power Generation*, vol.9, no.6, pp.593-599, 2015.

[15] M. H. Wang and Z. Y. Lee, Application of extension method and chaos theory in ECG identity recognition system, *IEEE the 14th International Conference on Industrial Informatics (INDIN)*, pp.1247-1251, 2016.